



## LiPF<sub>6</sub> and lithium difluoro(oxalato)borate/ethylene carbonate + dimethyl carbonate + ethyl(methyl)carbonate electrolyte for Li<sub>4</sub>Ti<sub>5</sub>O<sub>12</sub> anode

Hongming Zhou <sup>a,b</sup>, Zhenqi Fang <sup>a,\*</sup>, Jian Li <sup>a,b</sup>

<sup>a</sup> School of Materials Science and Engineering, Central South University, Changsha, Hunan 410083, China

<sup>b</sup> Hunan Zhengyuan Institute for Energy Storage Materials and Devices, Changsha, Hunan 410083, China

### HIGHLIGHTS

- ▶ Suitability between LiDFOB and Li<sub>4</sub>Ti<sub>5</sub>O<sub>12</sub> is presented.
- ▶ LiDFOB-based electrolyte shows highly interface stability to Li<sub>4</sub>Ti<sub>5</sub>O<sub>12</sub>.
- ▶ LiDFOB-based cells exhibit fairly well capacity retention after cycle at 60 °C.
- ▶ Internal resistance of LiDFOB cells increases slowly when it works at 60 °C.

### ARTICLE INFO

#### Article history:

Received 22 June 2012

Received in revised form

19 October 2012

Accepted 19 November 2012

Available online 27 November 2012

#### Keywords:

Lithium difluoro(oxalato)borate

Lithium titanate anode

Lithium-ion batteries

Electrolyte

### ABSTRACT

Lithium difluoro(oxalato)borate (LiDFOB) has been investigated as lithium salt for non-aqueous electrolytes for Li<sub>4</sub>Ti<sub>5</sub>O<sub>12</sub> anode in lithium-ion batteries. The electrolytes based on LiDFOB and carbonates are systematically investigated for LiFePO<sub>4</sub>/Li<sub>4</sub>Ti<sub>5</sub>O<sub>12</sub> cells, by scanning electron microscopy (SEM) analysis, inductively coupled plasma (ICP) analysis and various electrochemical tests, such as cyclic voltammetry (CV), linear sweep voltammetry (LSV), electrochemical impedance spectroscopy (EIS), and charge-discharge test. The results show that at 25 °C and 60 °C, the stability and Al collector corrosion-protection ability of LiDFOB-based electrolyte are superior to LiPF<sub>6</sub>-based electrolyte; The Li<sub>4</sub>Ti<sub>5</sub>O<sub>12</sub>/Li half-cells used LiDFOB or LiPF<sub>6</sub> as electrolyte salt have simple redox peaks, and their first charge-discharge curves have stable plateau. The differential of rate capability between LiDFOB battery and LiPF<sub>6</sub> battery with LiFePO<sub>4</sub>/Li<sub>4</sub>Ti<sub>5</sub>O<sub>12</sub> electrodes are not significant at 25 °C. LiDFOB battery exhibits better cycle performance than LiPF<sub>6</sub> battery, which is particularly remarkable at 60 °C. The stability of the Li<sub>4</sub>Ti<sub>5</sub>O<sub>12</sub> material in LiDFOB-based electrolyte is much better than that in LiPF<sub>6</sub>-based electrolyte at 60 °C.

© 2012 Elsevier B.V. All rights reserved.

## 1. Introduction

Lithium-ion batteries have been widely utilized as a power source for portable electronic devices [1,2]. Recently, much effort has been made to promote their application in hybrid electric vehicles and dispersed energy storage systems, which demand light weight, small volume, high energy density and highly security [3–5]. As a promising anode material for the lithium-ion batteries, spinel Li<sub>4</sub>Ti<sub>5</sub>O<sub>12</sub> exhibits many advantages compared to the currently used graphite [6,7]. For example, there is negligible change in the unit cell volume of Li<sub>4</sub>Ti<sub>5</sub>O<sub>12</sub> during lithium insertion and extraction, so it was named as zero strain material [8,9]. It also

has very wide voltage plateau at around 1.55 V vs. Li/Li<sup>+</sup>, which is higher than the reduction potential of most organic electrolytes. Therefore, Li<sub>4</sub>Ti<sub>5</sub>O<sub>12</sub> is much safer and more stable than carbon-based materials [10].

In 2006, lithium difluoro(oxalato)borate (LiDFOB) is first reported by Zhang [11] as a unique lithium salt for improved electrolyte of lithium-ion battery. Since LiDFOB has a part of similar structure as LiBOB [12–14], it is found that LiDFOB has the most of the unique characteristics of LiBOB in lithium-ion batteries. Furthermore, LiDFOB is superior to LiBOB in the properties as below: (1) it is more soluble in linear carbonate solvents that are essential to lower viscosity and provide the probability to optimize the solvents for the higher conductivity over a wide temperature range [15]; (2) it helps to form steady solid electrolyte interface (SEI) with less resistance, lithium-ion cell using this salt has better power capability and low temperature cyclic performance. These

\* Corresponding author. Tel./fax: +86 731 88877173.

E-mail address: [fzq880419@vip.qq.com](mailto:fzq880419@vip.qq.com) (Z. Fang).

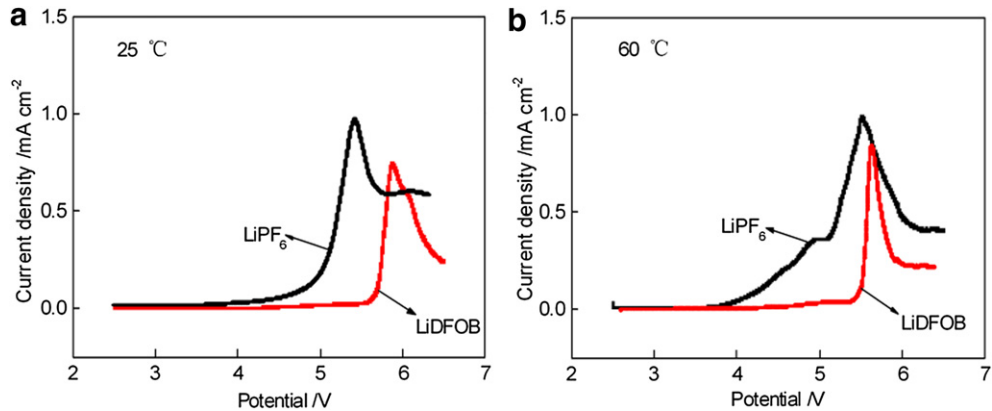


**Fig. 1.** Linear sweep voltammograms of 1 M LiDFOB (or LiPF<sub>6</sub>) in 1:1:1wt. EC/DMC/EMC electrolytes at (a) 25 °C and (b) 60 °C at the scan rate 1  $\text{mV s}^{-1}$ . The working and reference electrodes are Pt and lithium, respectively.

unique characteristics make LiDFOB as a promising salt for high-power applications [16,17].

Up to date, the electrochemical performances of LiDFOB in ethylene carbonate (EC)/propylene carbonate (PC)/ethylmethyl carbonate (EMC) or EC/dimethyl carbonate (DMC) solvent systems with some kinds of high-power lithium-ion cells were studied, such as LiNi<sub>0.8</sub>Co<sub>0.15</sub>Al<sub>0.05</sub>O<sub>2</sub>/graphite [18], Li<sub>1.1</sub>[Ni<sub>1/3</sub>Mn<sub>1/3</sub>Co<sub>1/3</sub>]<sub>0.9</sub>O<sub>2</sub>/graphite [19] and LiFePO<sub>4</sub>/graphite [16] cells. However, to the best of our knowledge, the electrochemical performances of LiDFOB-based electrolytes with LiFePO<sub>4</sub>/Li<sub>4</sub>Ti<sub>5</sub>O<sub>12</sub> battery, which is now popularly considered as the most promising one for using in large-scale lithium-ion batteries for HEV and EV applications, because of its low cost, safer performance and environmental benign nature, has not been shown in any document yet. It was for this purpose that we first systematically investigated LiDFOB, with the focus

placed on evaluating the resultant electrolytes in LiFePO<sub>4</sub>/Li<sub>4</sub>Ti<sub>5</sub>O<sub>12</sub> cells, compared with LiPF<sub>6</sub>-based electrolyte, which is widely used in lithium-ion battery [20,21], using various electrochemical techniques.

## 2. Experimental

### 2.1. Electrolyte preparation

LiPF<sub>6</sub> (battery degree) was purchased from Ferro Corporation (China). LiDFOB (battery degree) was provided by Hunan Zhen-gyuan Institute for Energy Storage Materials and Devices. EMC, EC and DMC were obtained from Shenzhen CAPCHEM Technology Co., Ltd., China. The electrolytes used in this work are 1.0 mol  $\text{L}^{-1}$  LiDFOB (LiPF<sub>6</sub>) in EC/DMC/EMC solvents (mass ratio of EC to DMC to

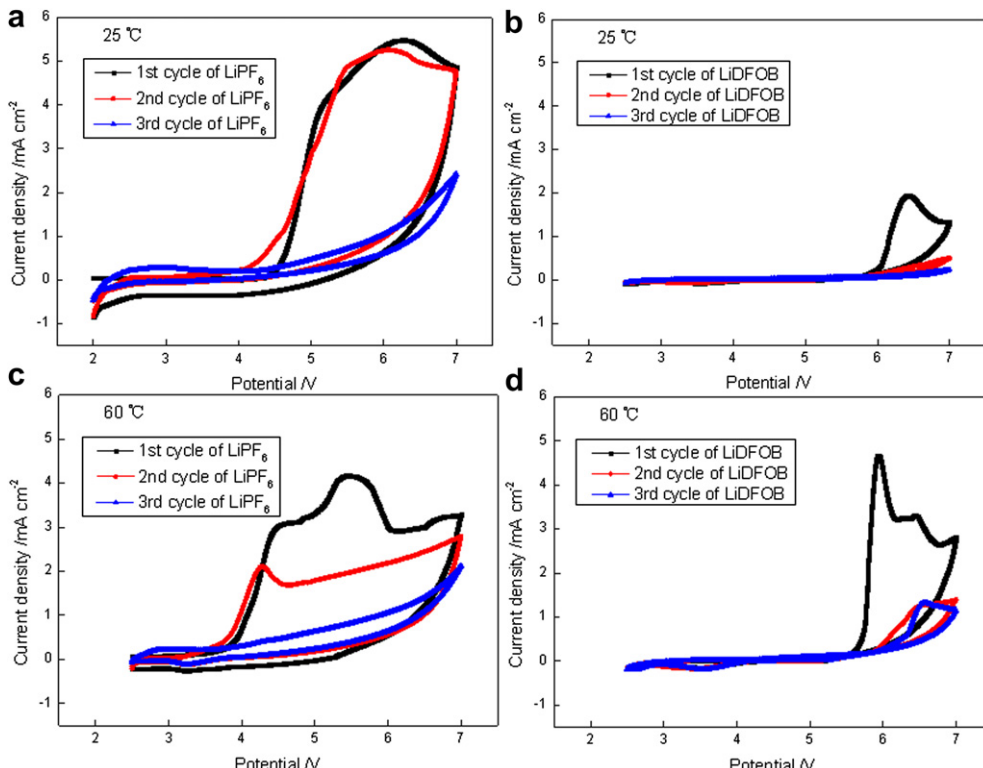


**Fig. 2.** CV curves of 1 M LiDFOB (or LiPF<sub>6</sub>) in 1:1:1wt. EC/DMC/EMC electrolytes to cathode current collector Al at (a), (b) 25 °C and (c), (d) 60 °C.

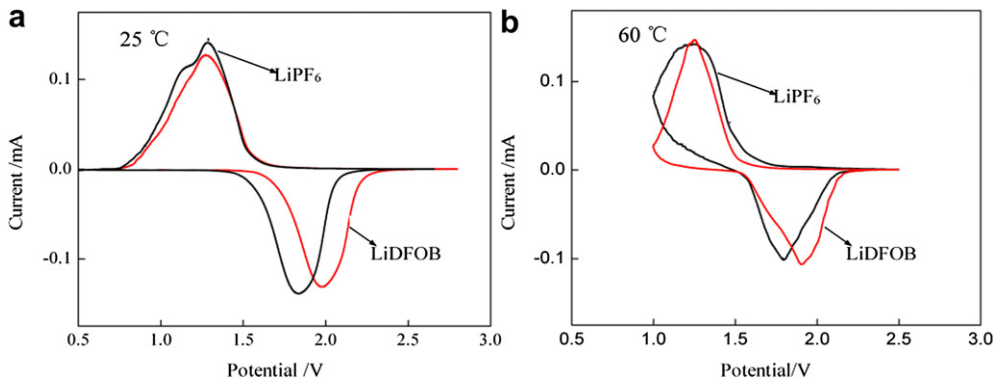


**Fig. 3.** Cyclic voltammetry curves of  $\text{Li}_4\text{Ti}_5\text{O}_{12}/\text{Li}$  half-cell using LiDFOB (or  $\text{LiPF}_6$ ) as electrolyte salt at (a)  $25\text{ }^\circ\text{C}$  and (b)  $60\text{ }^\circ\text{C}$ .

EMC is 1:1:1). All electrolytes were prepared in an argon-filled glove box (Universal 2440/750, Mikrouna Mech. Tech. Co., Ltd., Water content: <1ppm, oxygen content: <1 ppm). Water and free acid contents of the electrolytes were controlled below 20ppm, which were determined by Mettler Toledo DL32 titrator and Karl-Fisher 798 MPT Titrino, respectively.

## 2.2. Cell preparation

The  $\text{Li}_4\text{Ti}_5\text{O}_{12}/\text{Li}$  half-cells were assembled as CR2025 type coin cell in the argon-filled glove box using Celgard 2400 as separator. The working electrode was composed of 80 wt%  $\text{Li}_4\text{Ti}_5\text{O}_{12}$ , 10 wt% carbon black and 10 wt% polyvinylidene fluoride (PVdF). The electrode materials were evenly mixed and then attached on Al foils. The counter and reference electrodes were lithium tablets.

In order to investigate the corrosion behaviors between electrolyte and Al collection, Al foil and Li tablet were assembled as cathode and anode in a CR2025 type coin using Celgard 2400 as separator.

For full cell,  $\text{LiFePO}_4$  and  $\text{Li}_4\text{Ti}_5\text{O}_{12}$  were employed as cathode and anode which were separated by Celgard 2400 as well in 18650-type cells. The cathode electrode was composed of 80 wt%  $\text{LiFePO}_4$ , 10 wt% sodium carboxymethyl cellulose (CMC) and 10 wt% carbon black. The composition of anode electrode was the same as the  $\text{Li}_4\text{Ti}_5\text{O}_{12}$  electrode of half-cell above. The anode electrode and cathode electrode were all coated on Al foils.

## 2.3. Cyclic voltammetry and AC impedance measurements

In order to investigate the electrochemical behavior of LiDFOB in Li-ion battery, a CH Instrumental Electrochemical Workstation

(CHI6660) with a three-electrode system concluding  $\text{Li}_4\text{Ti}_5\text{O}_{12}$  and Pt as the working electrode respectively, and Li tablet as counter and reference electrodes was used for linear sweep voltammetry (LSV) at the scanning rate of  $0.1\text{ mV s}^{-1}$ . The voltages in this article were relative to  $\text{Li}/\text{Li}^+$ . Electrochemical impedance spectroscopy (EIS) measurements were also performed with a CH Instrumental Electrochemical Workstation (CHI6660). The batteries were tested in the frequency range from  $10\text{ mHz}$  to  $100\text{ kHz}$  with a perturbation amplitude of 5 mV. The charge-discharge performance of  $\text{LiFePO}_4/\text{Li}_4\text{Ti}_5\text{O}_{12}$  cell was tested by BTS0105C8 tester with a voltage range between  $1.5\text{ V}$  and  $2.8\text{ V}$  at  $0.2\text{ C}$ .

## 2.4. Characterization with scanning electron microscope (SEM)

The cells were taken apart after measured at  $60\text{ }^\circ\text{C}$ . Their electrodes were taken out and soaked in and rinsed with DMC to remove the remainder electrolyte. The electrodes morphologies after dried in a vacuum drier were observed by SIRION 200 SEM.

## 3. Results and discussion

### 3.1. Electrochemical stability window of the electrolytes

The electrochemical stability window of the electrolytes at  $25\text{ }^\circ\text{C}$  and  $60\text{ }^\circ\text{C}$  was investigated by using the linear sweep voltammetry (LSV) as shown in Fig. 1(a) and (b).

It is evident that the initial decomposition voltage of  $\text{LiPF}_6$ -based electrolyte and LiDFOB-based electrolyte is  $4.2\text{ V}$  and  $5.57\text{ V}$  respectively at  $25\text{ }^\circ\text{C}$  (Fig. 1a). With further increase of the potential, an obvious peak occurred in each curve. The voltage of the peak of LiDFOB-based electrolyte was  $5.87\text{ V}$ , which was higher than that

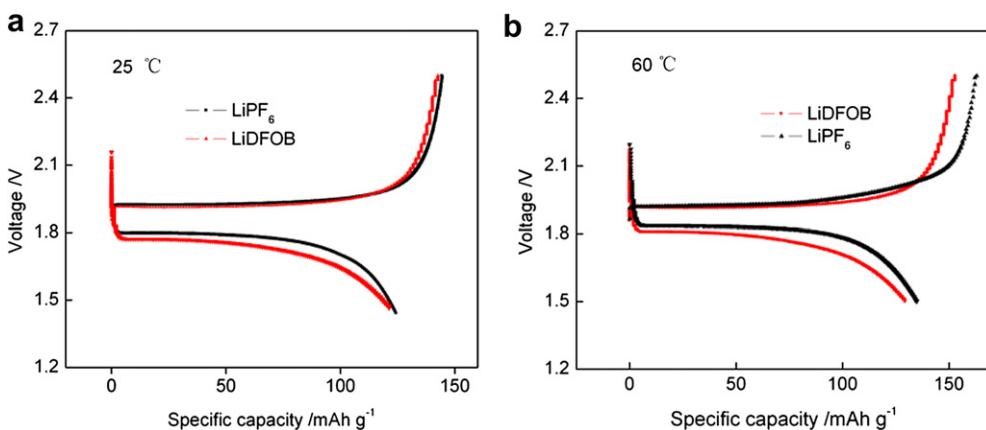


**Fig. 4.** The first charging and discharging curves of  $\text{LiFePO}_4/\text{Li}_4\text{Ti}_5\text{O}_{12}$  cell using 1 M LiDFOB (or  $\text{LiPF}_6$ ) in a 1:1:1wt. EC/DMC/EMC mixed solvent at (a)  $25\text{ }^\circ\text{C}$  and (b)  $60\text{ }^\circ\text{C}$ .

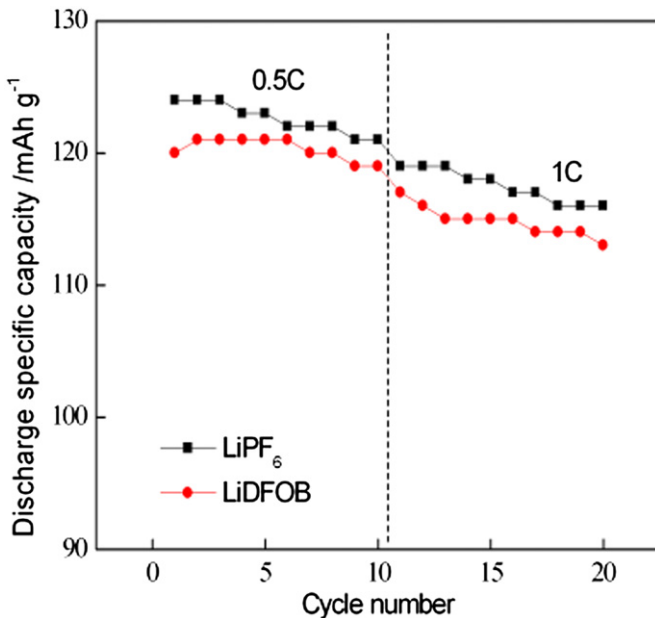


**Fig. 5.** Discharge capacity of  $\text{LiFePO}_4/\text{Li}_4\text{Ti}_5\text{O}_{12}$  cell using 1 M LiDFOB (or  $\text{LiPF}_6$ ) in a 1:1:1wt. EC/DMC/EMC mixed solvent at different discharge rates.

(5.4 V) of  $\text{LiPF}_6$ -based electrolyte. In another words, LiDFOB-based electrolyte had wider electrochemical stability window, which made it more suitable for high voltage battery.

At 60 °C, the initial decomposition voltage of  $\text{LiPF}_6$ -based electrolyte and LiDFOB-based electrolyte was 3.98 V and 4.2 V respectively. The oxidation current of  $\text{LiPF}_6$ -based electrolyte increased rapidly, which was attributed to that,  $\text{LiPF}_6$  decomposed into HF and  $\text{LiF}$  [22] when the voltage was around 3.98 V. It was about 5.7 V when the peak appeared which was believed to be solvent oxidization in the LiDFOB-based electrolyte. Based on the data above, we can conclude that LiDFOB-based electrolyte is more stable at high temperature. Moreover, the decomposition voltages of both kinds of electrolyte decreases with the temperature increasing, which indicates that the stability of electrolytes will get worse when they are working at higher temperature.

### 3.2. Interface stability between electrolyte and aluminum foil

The corrosion behaviors of LiDFOB-based or  $\text{LiPF}_6$ -based electrolyte on aluminum foil at different temperature are displayed in Fig. 2.

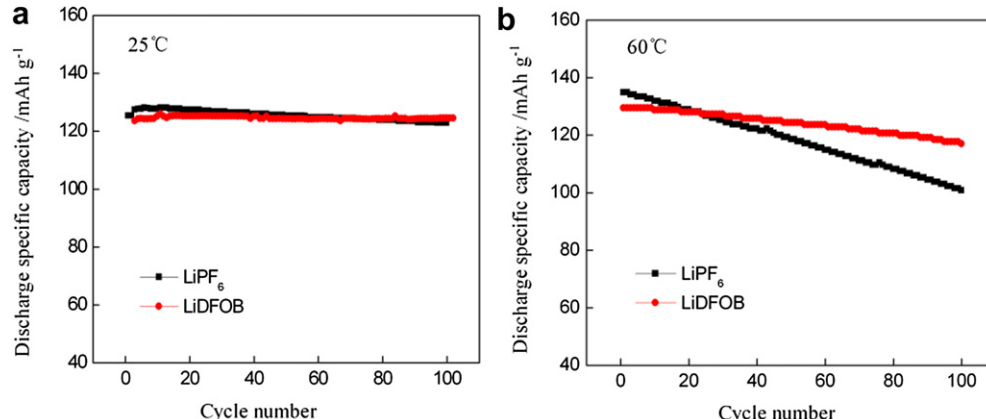


**Fig. 6.** Cycling performance of  $\text{LiFePO}_4/\text{Li}_4\text{Ti}_5\text{O}_{12}$  cell using 1 M LiDFOB (or  $\text{LiPF}_6$ ) in a 1:1:1wt. EC/DMC/EMC mixed solvent at charge and discharge rate 0.2 C. (a) 25 °C and (b) 60 °C.

The Fig. 2(a) and (b) showed that a slow increase of current occurred at 5.8 V and 4.55 V vs.  $\text{Li}^+/\text{Li}$  in the first positive sweep respectively for LiDFOB-based and  $\text{LiPF}_6$ -based electrolyte. The curve of  $\text{LiPF}_6$ -based electrolyte showed more than one peak during the positive sweep, which meant that the electrolyte decomposed and the products react with aluminum. Concerning LiDFOB-based electrolyte, the corrosion current was not obvious and the oxidation current occurred at higher potential. Though the peak height got lower in the second cycle, the oxidation peak of  $\text{LiPF}_6$ -based electrolyte occurred at lower potential. But the oxidation current of LiDFOB-based electrolyte did not occur until the potential closed to 6V. The reduction peak during the negative sweep in these curves is small. So that we can conclude that the oxidation reactions were irreversible. The measurements above shows that LiDFOB-based electrolyte has better interface stability to Al at 25 °C than  $\text{LiPF}_6$ -based electrolyte.

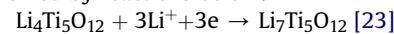
The data given in Fig. 2(c) and (d) show a different phenomenon in the test at 60 °C. Comparing to the LSV curve, the oxidation current peaks of LiDFOB-based electrolyte were obvious in the first positive sweep. That was partly because the decomposition of electrolyte and partly because the reaction between the decomposition products and aluminum. In the second cycle, the curve showed a single current peak again, and the peak occurred at a 0.5 V higher potential than it in the first sweep. In the case of  $\text{LiPF}_6$ , although there were three current peaks in the curve of the first sweep either, the area of peak was much larger than that of LiDFOB-based electrolyte, and the peak occurred at lower potential. The curves of second cycle showed a similar trend to the result tested at 25 °C. Because of its poor corrosion-protection ability, the  $\text{LiPF}_6$ -based electrolyte eroded the Al collection when the voltage closed to a lower level during the second sweep. We can conclude that LiDFOB, a promising alternative salt for  $\text{LiPF}_6$ , can undertake higher voltage at 60 °C.

Comparing Fig. 2(a) and (b), a further conclusion can be drawn that the interface stability of electrolyte to Al at 25 °C is better than it at a higher temperature.

### 3.3. Cyclic voltammetry curves of $\text{Li}_4\text{Ti}_5\text{O}_{12}/\text{Li}$ half-cell

Cyclic voltammetry curves of the  $\text{Li}_4\text{Ti}_5\text{O}_{12}/\text{Li}$  half-cell at 25 °C and 60 °C are plotted in Fig. 3(a) and (b).

It is obvious that all kinds of curves of half-cells mentioned above have only one peak pair, containing one oxidation peak and one reduction peak, which corresponds to the intercalation and extraction of Li-ion. The oxidation and reduction processes can be showed by reactions below:





All the shapes of the pairs of oxidation peak and reduction peak are similar and narrow, and the peak intensities are strong. At 25 °C, the oxidation and reduction processes of cells using LiDFOB as electrolyte salt occurred at 1.98 V and 1.38 V, respectively. The corresponding processes of LiPF<sub>6</sub>-based cell occurred at 1.86 V and 1.40 V, respectively. The processes of both kind of cells occurred at a little lower potential when the temperature increased to 60 °C. According to the common electrochemical knowledge, it means that those reactions are reversible. The potential separation between the anodic and cathodic peaks can also affect to the kinetics characteristics at a certain extent. But the difference of the potential separation between LiDFOB-based electrolyte and LiPF<sub>6</sub>-based electrolyte is small. This indicated that, with LiDFOB and LiPF<sub>6</sub> electrolyte, Li<sub>4</sub>Ti<sub>5</sub>O<sub>12</sub>/Li half-cells had good reversibility of the reaction. Therefore, both LiDFOB and LiPF<sub>6</sub> are friendly to Li<sub>4</sub>Ti<sub>5</sub>O<sub>12</sub> electrode.

#### 3.4. The charge-discharge performance of LiFePO<sub>4</sub>/Li<sub>4</sub>Ti<sub>5</sub>O<sub>12</sub> cell

The initial charging and discharging performance of cells, using 1 M LiDFOB (or LiPF<sub>6</sub>) in a 1:1:1wt. EC/DMC/EMC mixed solvent at 25 °C and 60 °C, were exhibited in Fig. 4.

At 25 °C or 60 °C, LiDFOB and LiPF<sub>6</sub> cells had much similar voltage-capacity correlations and stable charging and discharging plateau, which meant that LiDFOB-based electrolyte had good compatibility with Li<sub>4</sub>Ti<sub>5</sub>O<sub>12</sub>. There were very similar cycling efficiencies of the first cycles for LiDFOB and LiPF<sub>6</sub> cells at 25 °C, which were 85.1% and 86.2% respectively. At 60 °C the cycling efficiency of LiDFOB cell was higher than that of LiPF<sub>6</sub> cell, which indicated that the LiPF<sub>6</sub> had the tendency to decompose into HF and LiF. Solid LiF particles may move to the separator with ions and block the micropores to encumber the transport of Li-ion. HF would damage the electrode material, and let the capacity down directly. In comparison, LiDFOB had a little smaller conductivity but much better stability which brought the cell larger capacity. Therefore, we may conclude, at 25 °C both LiDFOB and LiPF<sub>6</sub> are suitable for Li-ion cell from the capacity aspect. But LiDFOB cell has better performance when the cell works at 60 °C.

The rate capabilities of LiFePO<sub>4</sub>/Li<sub>4</sub>Ti<sub>5</sub>O<sub>12</sub> cells were shown in Fig. 5. The specific discharge capacities gradually decreased with increasing the applied current densities for both the cells. The relative capacities of two kinds of cell were nearly the same at 25 °C. The capacity of cell using LiPF<sub>6</sub> was a little bit higher, which was due to the higher conductivity of LiPF<sub>6</sub>.

Fig. 6(a) presents the impact of the two salts on cycling performance of LiFePO<sub>4</sub>/Li<sub>4</sub>Ti<sub>5</sub>O<sub>12</sub> cells at 25 °C. It can be seen from Fig. 6, the LiFePO<sub>4</sub>/Li<sub>4</sub>Ti<sub>5</sub>O<sub>12</sub> cell using LiPF<sub>6</sub> as electrolyte salt initially delivered 127.6 mAh g<sup>-1</sup> and retained 121.6 mAh g<sup>-1</sup> at the 100th cycle. However, when LiDFOB was used as the lithium salt in the electrolyte, the LiFePO<sub>4</sub>/Li<sub>4</sub>Ti<sub>5</sub>O<sub>12</sub> cell initially delivered 124.7 mAh g<sup>-1</sup> and retained 123.3 mAh g<sup>-1</sup> at the 100th cycle, the discharge capacity for LiDFOB was able to retain about 98.9%, higher than that (95.3%) of LiPF<sub>6</sub>. Thus, the cycling performance of the cells using LiDFOB as lithium salt in electrolyte was better than the cells that using LiPF<sub>6</sub> as lithium salt.

Cycling performance of the LiFePO<sub>4</sub>/Li<sub>4</sub>Ti<sub>5</sub>O<sub>12</sub> cells at high temperature was also evaluated. After 100 cycles at 60 °C, comparisons of different discharge capacities are summarized in Fig. 6(b), the discharge capacity retention was 74.7% and 90.3% for LiPF<sub>6</sub> and LiDFOB, respectively. The lost of the capacity of LiPF<sub>6</sub> cell attributed to the decomposition of the LiPF<sub>6</sub> as well. All the data above indicated that, the charge-discharge efficiencies of LiDFOB cell and LiPF<sub>6</sub> cell were both superior at 25 °C. Besides, the efficiency and the stability of LiDFOB cell were much better than those of LiPF<sub>6</sub> cell at 60 °C.

#### 3.5. Impedance analysis

We attempted to observe AC impedance changes of the cells, and to understand the resistance of the interface film formed on the electrode surface. The cells were measured before and after 100 cycles at 25 °C and 60 °C respectively. The impedance spectra of the Li<sub>4</sub>Ti<sub>5</sub>O<sub>12</sub>/Li cells containing the two different electrolytes were shown in Fig. 7.

All EIS curves were consisted of two parts: a semicircle at high and medium frequency, which reflected the charge-transfer reaction resistance  $R_{ct}$ , and a sloping line at the low frequency, which gave expression to the Li-ion diffusion into the active mass. It suggested that the surface film was not formed yet, because of the absence of passive film resistance and its relative capacitance. With the temperature increasing from 25 °C to 60 °C, impedances of all the cells decreased greatly. This was attributed to the increase of conductivity of electrolyte at higher temperature, and the Li-ion moves faster through cathode which makes the Li-ion easier to deintercalate.

Fig. 7(a) indicated that the electrolyte resistance  $R_L$  and charge-transfer reaction resistance  $R_{ct}$  of LiDFOB cell and LiPF<sub>6</sub> cell increased respectively after 100 cycles at 25 °C (Fig. 7a).

Fig. 7(b) showed that, after 100 cycles, both  $R_L$  and  $R_{ct}$  increased at 60 °C too. But due to the instability of LiPF<sub>6</sub>, the impedance of LiPF<sub>6</sub> cell increased obviously. In contrast, because the LiDFOB was

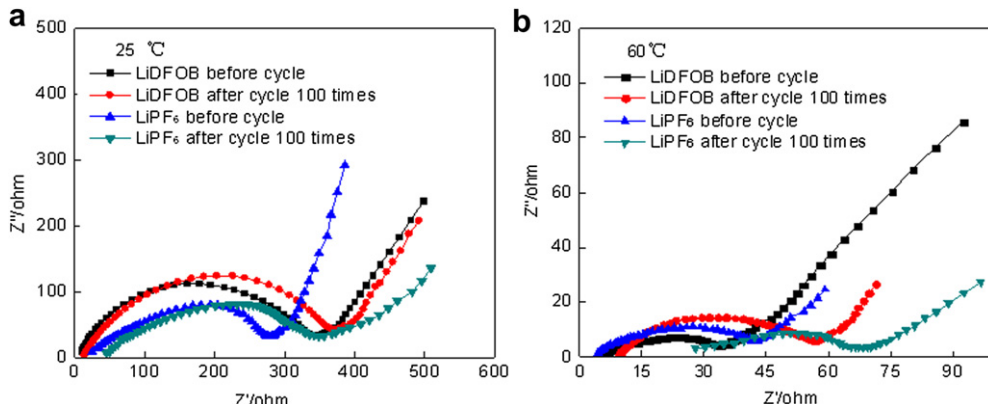
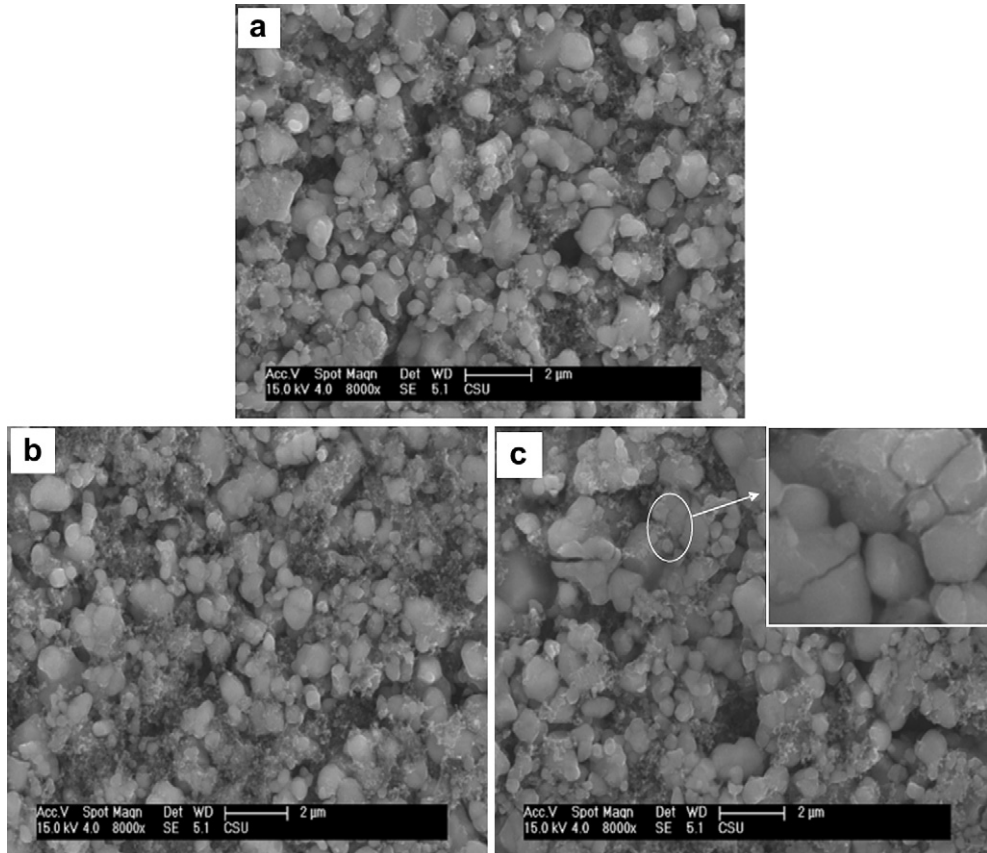


Fig. 7. Electrochemical impedance spectra of Li<sub>4</sub>Ti<sub>5</sub>O<sub>12</sub>/Li cells using 1 M LiDFOB (LiPF<sub>6</sub>) in a 1:1:1wt. EC/DMC/EMC mixed solvent before and after 100 cycles at (a) 25 °C and (b) 60 °C.



**Fig. 8.** SEM images of LiFePO<sub>4</sub> electrode from LiFePO<sub>4</sub>/Li<sub>4</sub>Ti<sub>5</sub>O<sub>12</sub> cells at 60 °C (a) before cycle, (b) LiDFOB-based electrolytes and (c) LiPF<sub>6</sub>-based electrolytes.

more stable at that temperature, the increase of impedance was invisible and much slower. Therefore, though its impedance was a little larger at 25 °C, LiDFOB cell had superior cycling performance and little impedance at high temperature.

### 3.6. Surface morphology of LiFePO<sub>4</sub> electrode before and after cycles at high temperature

Fig. 8 showed the SEM images of the LiFePO<sub>4</sub> electrodes taken from the cells with the two electrolytes, which cycled at high temperature, respectively.

It can be seen from Fig. 8 that, after 100 cycles some of the LiFePO<sub>4</sub> particles in the LiPF<sub>6</sub>-based cell were cracked (Fig. 8c). That was attributed to the corrosion by HF (from the decomposition of LiPF<sub>6</sub>) and the solution of the corrosion products. However, the corrosion of LiDFOB-based electrolytes on LiFePO<sub>4</sub> was low and the stability was good at high temperature. Therefore, the images of LiFePO<sub>4</sub> particles in LiDFOB-based cell after 100 cycles were almost the same as that before cycle. This indicated that LiDFOB electrolyte was not able to erode the LiFePO<sub>4</sub> electrode.

### 3.7. ICP analysis

In order to understand the chemical stability of the Li<sub>4</sub>Ti<sub>5</sub>O<sub>12</sub> in the two electrolytes, we tested the content of Ti<sup>4+</sup> in different Li<sub>4</sub>Ti<sub>5</sub>O<sub>12</sub> powder/electrolytes after standing at 60 °C for one week. The amount of Ti-ions dissolved from Li<sub>4</sub>Ti<sub>5</sub>O<sub>12</sub> in the two different electrolytes was compared in Fig. 9.

Obviously, 10.8 ppm of Ti-ions was detected in LiPF<sub>6</sub>-based electrolyte, while less than 0.3 ppm of Ti-ions were dissolved in the case of LiDFOB-based electrolyte. The dissolution of Ti-ions from

crystal into the electrolyte was due to the disproportionation on the surface of the electrode, caused by HF attack generated by fluorine from PF<sub>6</sub> and protons from electrolyte impurities, at high temperature. The result illuminated that in spite of the presence of fluorine in LiDFOB, it did not generate a mass of HF to erode Li<sub>4</sub>Ti<sub>5</sub>O<sub>12</sub> electrode at high temperature.

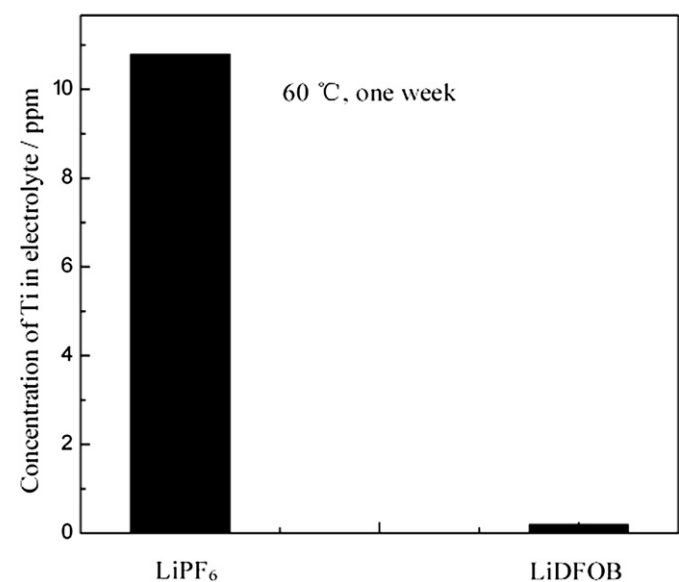


**Fig. 9.** Concentration of Ti<sup>4+</sup> ions dissolved from Li<sub>4</sub>Ti<sub>5</sub>O<sub>12</sub> powder stored in 1.0 M LiPF<sub>6</sub>/EC:PC:EMC (1:1:1) and 1.0 M LiDFOB/EC:PC:EMC (1:1:1) for one week at 60 °C.

#### 4. Conclusions

LiDFOB was investigated as an alternative lithium salt to LiPF<sub>6</sub> in electrolyte used in Li-ion cells. According to this research, the electrochemistry performance of LiDFOB cell is better than LiPF<sub>6</sub> cell. What is more important, LiDFOB has superior stability at high temperature.

In the CV and initial cycling curves of Li<sub>4</sub>Ti<sub>5</sub>O<sub>12</sub>/Li half-cell, we found that both LiDFOB and LiPF<sub>6</sub> half-cells had single pair of oxidation-reduction peaks and stable charge-discharge plateau. That is to say, both kinds of electrolyte are friendly to Li<sub>4</sub>Ti<sub>5</sub>O<sub>12</sub> electrode.

Analyzing cycling performance curves of LiFePO<sub>4</sub>/Li<sub>4</sub>Ti<sub>5</sub>O<sub>12</sub> cells, we concluded that the capacity retention of LiDFOB cell after 100 cycles was 90.3%, much higher than the LiPF<sub>6</sub> cell 74.7% capacity retention at 60 °C, though their capacity retentions were merely equal at 25 °C. The capacity retention will rise by using LiDFOB instead of LiPF<sub>6</sub>.

The increment of impedance of LiDFOB cell after 100 cycles at 60 °C is significantly smaller than the increment of LiPF<sub>6</sub> cell's impedance, according to the EIS. Analyzing the SEM image, we noticed that many of particles of LiFePO<sub>4</sub> using LiPF<sub>6</sub> as electrolyte salt cracked after 100 cycles at 60 °C. But the cracks were hardly to find on the counterpart of LiDFOB cell. Cell systems using LiDFOB are safer and more stable at high temperature.

#### Acknowledgments

Financial support from the Science and Technology Project of Hunan Province, Granted No. 2010FJ4061 and the Science and

Technology Project of Changsha, Granted No. k1201039-11 are gratefully acknowledged.

#### References

- [1] A. Ritchie, W. Howard, *J. Power Sources* 162 (2006) 809–812.
- [2] J. Yamaki, *Encyclopedia of Electrochem. Power Sources* (2009) 183–191.
- [3] J.V. Mierlo, P.V. den Bossche, G. Maggetto, *J. Power Sources* 128 (2004) 76–89.
- [4] J. Arai, T. Yamaki, S. Yamauchi, T. Yuasa, T. Maeshima, T. Sakai, M. Koseki, T. Horiba, *J. Power Sources* 146 (2005) 788–792.
- [5] S. Beninati, L. Damen, M. Mastragostino, *J. Power Sources* 194 (2009) 1094–1098.
- [6] T.-F. Yi, L.-J. Jiang, J. Shu, C.-B. Yue, R.-S. Zhu, H.-B. Qiao, *J. Phys. Chem. Solids* 71 (2010) 1236–1242.
- [7] I. Belharouak, G.M. Koenig Jr., K. Amine, *J. Power Sources* 196 (2011) 10344–10350.
- [8] K.-C. Hsiao, S.-C. Liao, J.-M. Chen, *Electrochimica Acta* 53 (2008) 7242–7247.
- [9] Z.-G. Wang, W.-J. Peng, Z.-X. Wang, X.-H. Li, H.-J. Guo, L. Wu, T. Nonferr. Metal. Soc. 20 (2010) s271–s274.
- [10] L. Cheng, H.-J. Liu, J.-J. Zhang, *J. Electrochem. Soc.* 153 (2006) A1472–A1477.
- [11] S.S. Zhang, *Electrochem. Commun.* 8 (2006) 1423–1428.
- [12] S.S. Zhang, K. Xu, T.R. Jow, *J. Solid State Electr.* 7 (2003) 147.
- [13] S.S. Zhang, K. Xu, T.R. Jow, *Electrochem. Commun.* 4 (2002) 928.
- [14] K. Xu, S.S. Zhang, U. Lee, J.L. Allen, T.R. Jow, *J. Power Sources* 146 (2005) 79.
- [15] M.H. Fu, K.L. Huang, S.Q. Liu, L.S. Liu, Y.K. Li, *J. Power Sources* 195 (2010) 862–866.
- [16] Z.-A. Zhang, X.-J. Chen, F.-Q. Li, Y.-Q. Lai, J. Li, P. Liu, X.-Y. Wang, *J. Power Sources* 195 (2010) 7397–7402.
- [17] H.-Q. Gao, Z.-A. Zhang, Y.-Q. Lai, *J. Cent. South Univ. Technol.* 15 (2008) 830–834.
- [18] X. Ang, Y. Li, B.L. Lucht, K. Sun-Ho, D.P. Abraham, *J. Electrochem. Soc.* 156 (2009) A318–A327.
- [19] Z.H. Chen, Y. Qin, J. Liu, K. Amine, *Electrochem. Solid St.* 12 (2009) A69–A72.
- [20] S.S. Zhang, K. Xu, T.R. Jow, *J. Power Sources* 159 (2006) 521–525.
- [21] X.-Z. Liao, Z.-F. Ma, Q. Gong, Y.-S. He, L. Pei, L.-J. Zeng, *Electrochem. Commun.* 10 (2008) 691–694.
- [22] H. Yang, Guorong V. Zhuang, Philip N. Ross Jr., *J. Power Sources* 161 (2006) 573–579.
- [23] T. Ohzuku, A. Ueda, *Solid State Ionics* 69 (1994) 201–211.